Mutational analysis of gene function in the *Anaplasmataceae*: Challenges and perspectives

Adela S. Oliva Chávez[a,*], Michael J. Herron[b], Curtis M. Nelson[b], Roderick F. Felsheim[b], Jonathan D. Oliver[c], Nicole Y Burkhardt[b], Timothy J. Kurtti[b], Ulrike G. Munderloh[b]

[a] *Department of Microbiology and Immunology, University of Maryland School of Medicine, Baltimore, MD, USA*
[b] *Department of Entomology, University of Minnesota, St. Paul, MN, USA*
[c] *School of Public Health, Division of Environmental Health Sciences, University of Minnesota, Minneapolis, MN, USA*

A B S T R A C T

Mutational analysis is an efficient approach to identifying microbial gene function. Until recently, lack of an effective tool for *Anaplasmataceae* yielding reproducible results has created an obstacle to functional genomics, because surrogate systems, e.g., ectopic gene expression and analysis in *E. coli,* may not provide accurate answers. We chose to focus on a method for high-throughput generation of mutants via random mutagenesis as opposed to targeted gene inactivation. In our search for a suitable mutagenesis tool, we considered attributes of the Himar1 transposase system, i.e., random insertion into AT dinucleotide sites, which are abundant in *Anaplasmataceae*, and lack of requirement for specific host factors. We chose the *Anaplasma marginale tr* promoter, and the clinically irrelevant antibiotic spectinomycin for selection, and in addition successfully implemented non-antibiotic selection using an herbicide resistance gene. These constructs function reasonably well in *Anaplasma phagocytophilum* harvested from human promyelocyte HL-60 cells or *Ixodes scapularis* tick cells. We describe protocols developed in our laboratory, and discuss what likely makes them successful. What makes *Anaplasmataceae* electroporation competent is unknown and manipulating electroporation conditions has not improved mutational efficiency. A concerted effort is needed to resolve remaining problems that are inherent to the obligate intracellular bacteria. Finally, using this approach, we describe the discovery and characterization of a putative secreted effector necessary for *Ap* survival in HL-60 cells.

1. Introduction

The family *Anaplasmataceae* includes important human and animal pathogens that are transmitted by ticks (Eremeeva and Dasch, 2011). The incidence of diseases caused by these bacteria has been increasing, likely due to the expanding range of tick vectors linked to global environmental changes such as warming temperatures, more humid weather patterns in endemic regions of the northern hemisphere, and human encroachment on tick host habitat. In combination, these factors support earlier and longer seasonal tick activity and greater chances of tick encounters by humans and companion animals (Robinson et al., 2015). In addition, human activities involved in animal trade and travel have resulted in the introduction of exotic tick-borne pathogens and exotic ticks into regions that were previously unaffected (Barre et al., 2011; ProMED-Mail, 2017).

Anaplasmoses and ehrlichioses are diseases that can be treated with a course of tetracycline antibiotics, but timing is important. When treatment is delayed, the illness can progress to a life-threatening pro-inflammatory syndrome in over one third of patients (Dahlgren et al., 2015; Schotthoefer et al., 2017). Immune-based prevention of these potentially life-threatening illnesses is a desirable goal, but none are currently available. Immunity against obligate intracellular bacteria involves cellular responses that are required for survival of an initial infection. In the case of *Anaplasma phagocytophilum* (*Ap*), the clearance of bacteria during primary infection in murine models is dependent on NK cells and IFN-γ and IL-12 secretion during early stages of infection followed by MHC II CD4 + T cell responses (Birkner et al., 2008). However, immune clearance of bacteria upon subsequent challenge

relies on antibodies produced by memory B-cells (Feng et al., 2004; Valbuena et al., 2004).

Outer membrane fractions or killed vaccines against the bovine pathogen *Anaplasma marginale* have been shown to induce protection from infection with homologous but not heterologous strains (Noh et al., 2008). In Israel and Australia, cattle are routinely vaccinated with the related, mild pathogen *Anaplasma centrale,* which is not approved for use in the US because it results in persistent infection and can cause clinical disease in vaccinees. Nevertheless, there is evidence that transient or long-term infection with vaccine strains may be necessary to achieve protective immunity against challenge with virulent *Anaplasmataceae*. For instance, an avirulent strain of *Ehrlichia muris* that causes inapparent, chronic infections in mice efficiently protects against fatal disease from the *Ixodes ovatus* ehrlichia (Thirumalapura et al., 2009), and specific mutants of other intracellular bacterial pathogens with an infection-deficient phenotype have been shown to protect against virulent wild-type challenge (Bao et al., 2017). *Anaplasma marginale* transposon mutants expressing fluorescent markers, including one with an insertion in the upstream region of an operon encoding several outer membrane proteins thought to be required for intracellular invasion, exhibited reduced infectivity for cattle without inducing disease. These mutants protected against challenge, and might thus be vaccine candidates (Crosby et al., 2015; Felsheim et al., 2010; Hammac et al., 2013). With the recent advances in mutagenesis of *Anaplasmataceae*, protective, live attenuated and safe vaccines based on specific mutants with decreased infection ability can now be pursued.

There are two major approaches to mutagenesis, targeted and random, and each poses distinct advantages and challenges. Targeted mutagenesis of known genes may be a quick route to disrupt gene function and identify deficient phenotypes suitable as, e.g., vaccine candidates. On the other hand, random mutagenesis is suited for high-throughput genome-scale gene analysis. In the *Rickettsiales,* as many as 45% of genes encode hypothetical proteins without known function (Rikihisa, 2011). This significantly restricts the number of targets that can rationally be chosen for directed mutagenesis, though hypothetical genes may encode proteins of critical importance. Bioinformatics-based analyses may aid in the identification of desirable targets, but are often unreliable when applied to *Rickettsiales*. Importantly, because of their uniqueness, hypothetical proteins constitute desirable choices for development of therapeutics or preventive therapies that are predicted to have few or no off-target or side effects. Here, we summarize and discuss the current status of random mutagenesis of the *Anaplasmataceae*. We present the methodology that has been most successful in our experience for the generation of random mutants. We analyze the characteristics of one such mutant that suffered a disruption in the coding region for a predicted effector at the locus APH_0906, corresponding to HGE1_03857. We present the results as an example of the power of random mutagenesis for the discovery of proteins involved in infection.

2. Background/history

Mutagenesis of obligate intracellular bacteria has been a goal pursued by a number of laboratories for decades, but has resisted routine application until recently. A variety of approaches were pursued early on, including allelic exchange and transposon mutagenesis. However, reports of successful mutagenesis techniques only started to accumulate at a faster rate in 2009, although the reasons for this uptick are not entirely clear (McClure et al., 2017). A system for extracellular cultivation of *Coxiella* provided a breakthrough that enabled the generation of a large number of mutants, highlighting the absolute need for a host cell as a major problem hindering mutagenesis in truly obligate intracellular bacteria (Beare et al., 2012). Another impediment for development of genetic systems for *Anaplasmataceae* remains the fact that these organisms, unlike the *Rickettsiaceae* (Burkhardt et al., 2011), are unable to maintain plasmids (unpublished), and are at this time not candidates for transformation with a shuttle vector, which is a standard

approach used to test bacterial gene function. Between 1994 and 2005, five publications appeared that describe successful events of transformation by non-specific DNA uptake and by transposon mutagenesis, including of typhus group rickettsiae (McClure et al., 2017). These successes were not generally adopted, in part because of the difficulties of working under BSL3 containment, and because conditions favoring transformation were not yet defined. Indeed, to date it is unknown what constitutes the state of transformation competence in *Anaplasmataceae*, and how to induce it. In 2006, Himar1 transposon mutagenesis was adapted to obtain stable mutants of *Ap*, a method which targets TA dinucleotides that are plentiful in their genomes, and does not require additional host factors for successful completion (Felsheim et al., 2006; Lampe et al., 1998). Subsequently, this work led to the generation of an *Ap* mutant library comprising over 1100 mutants. This library is currently being characterized to prepare it for distribution to the research community (Herron et al., 2010).

Recently, targeted mutagenesis of *Ehrlichia chaffeensis* using allelic exchange has been developed, and offers a direct way to address the function of a single gene (Wang et al., 2017), including even reconstitution of function. However, here we focus on transposon mutagenesis. In combination, these approaches ring in a new era of genome analysis for the *Anaplasmataceae* that has application to the *Rickettsiales* in general.

3. Approach and methods

3.1. Preparation of Anaplasmataceae for genetic transformation

Important considerations to take into account when working with obligate intracellular bacteria are 1) how to minimize damage while purifying them from their host cells in preparation of genetic manipulation, and 2) how to maintain their viability while extracellular. The obligate intracellular *Anaplasmataceae* quickly lose infectivity when kept outside host cells, thus minimizing this state is important. *Anaplasmataceae* lack a rigid cell wall that is devoid of peptidoglycan and lipopolysaccharide (Lin and Rikihisa, 2003). In our experience, washing extracellular *Anaplasmataceae* bacteria in PBS compromises their integrity, possibly by attacking their cell wall, and with each washing step, investigators are left with fewer, more damaged bacteria. Instead, sucrose solutions appear to be less aggressive, and are additionally suitable as a medium for electroporation of the bacteria. Even so, washing cell-free bacteria is detrimental in our experience (based on recovery of mutants), and should be avoided to the extent possible in order to maximize the number of mutants that can be recovered, whether they are derived from mammalian or tick cells. Nevertheless, a protocol for targeted gene disruption of *E. chaffeensis* by allelic exchange that was recently published (Wang et al., 2017) involves washing bacteria twice in 300 mM sucrose, and gives rise to mutants within two weeks. This approach does not require maximization of mutant yield, however, and presumably a single mutant should suffice to grow into a detectable population when under selection.

An effective protocol (Table 1) then takes a minimum amount of time and requires minimal manipulation of the bacteria. Accordingly, the protocol that our lab has used most successfully involves collecting infected host cells by centrifugation at room temperature, and lysing them mechanically by vortexing in ~1.5 ml of 300 mM sucrose in the presence of ~100 μl rock tumbler grit (60/90 silicon carbide grit, Lortone, Mukilteo, WA) followed by filtration through 2 μm pore size filters (Whatman Puradisc syringe filters). Bacteria are then centrifuged at 10–11,000 x *g* for 10 min, also at room temperature, and no additional washing steps are done. Bacterial pellets are resuspended in 300 mM sucrose with 1 μg of plasmid DNA, and incubated on ice for 15–20 min prior to electroporation, as described in Table 1.

Table 1
Protocol for the transformation of *Anaplasma* sp. bacteria.

Step	Procedure	Volume	Centrifugation speed (xg)	Temperature	Time (min)
1	Collect infected cells (above 90%)	Variable	350	RT	5
2	Resuspend cells in 300 mM sucrose	3 ml	–	RT	–
3	Add suspension into 2-ml microfuge tubes preloaded with silicone carbide tumbler grit 60/90 grade	50-100 μl	–	RT	–
4	Vortex tubes on high to disrupt host cells	–	–	RT	0.5
5	Twist a 2-μm pore size filter onto the barrel of a 5-ml syringe	–	–	RT	–
6	Remove supernatant, add to syringe and filter supernatant into 2-ml microfuge tubes	Variable	–	RT	–
7	Collect bacteria	Variable	10,000	RT	10
8	Resuspend bacteria in desired volume of sucrose	Variable	–	RT	–
9	Add 1-3 μg plasmid and transfer to electroporation cuvette	Variable	–	RT	–
10	Incubate on ice	Variable	–	4-6 °C	15
11	Electroporate at 400 Ohm, 25 μF, 1.8 kV (Pulse times should be 6-9 ms)	–	–	RT	–
12	Immediately recover bacteria in FBS	0.3 ml	–	RT	–
13	Mix with host cells (HL-60 or ISE6 cells) in culture media for the desired number of microplates	1.5 ml (or as needed)	–	RT	–
14-1	Incubate with host cells (HL-60)	1.5 ml (or as needed)	–	37 °C	60
14-2	Centrifuge suspension (ISE6)	1.5 ml (or as needed)	5000	RT	5
14-3	Incubate tubes with cell/bacteria pellet (ISE6)	1.5 ml (or as needed)	–	30 °C	120
15	Dilute cells in media for desired number of microplates	Variable	–	RT	–
16	Add spectinomycin and streptomycin the next day	Variable	–	RT	–

3.2. Electroporation and infection of host cells

Electroporation parameters that we have successfully used are 1.7–1.8 kV, 25 μF and 400 Ω, yielding a pulse of 7–9 ms (Felsheim et al., 2006). Bacteria are recovered from the cuvette in fetal bovine serum (FBS), and immediately added to host cells concentrated into a minimal volume of culture medium (1–1.5 ml with 10^7 HL-60 or ISE6 cells). Mammalian target cells are incubated with occasional gentle agitation at 37 °C for about 90 min before being seeded into 96-well plates and incubated at 37 °C with 5% CO_2 in humidified air. Bacteria mixed with tick cells are centrifuged at 5000 x *g* for 5 min at room temperature, and then incubated as a pellet at 30 °C for 90 min before seeding into 48 - or 96 -well plates that are incubated at 34 °C with 4% CO_2 in humidified air. Selecting agents are added after 5 h, or the next day. We most commonly use constructs encoding *aadA*, which confers resistance to spectinomycin and streptomycin, because it is rarely used clinically. Effective concentrations for selection should be tested beforehand, but 100 μg/ml is a good starting point. During electroporation, the bacterial cell membrane is altered structurally, presumably resulting in formation of pores that facilitate uptake of DNA. When successful, electroporation causes bacteria to clump, likely due to the effect on their cell membrane. Consequently, dilution of the cells that were incubated with electroporated bacteria into multi-well plates may result in introduction of more than one mutated bacterium (if caught together in a clump) into a single well, which is what we have experienced. Using this protocol with HL-60 cells results in recovery of ∼100 mutants each time, whereas with tick cells, the recovery of mutants is about 30–40 mutants from an infected ISE6 culture containing 10^7 infected cells, but can be much lower. In HL-60 cells, evidence of mutants expressing fluorescent markers can usually be observed within a week, whereas it takes about 2 weeks before the first mutants are detected in tick cells. Because tick cell culture plates are maintained for 4 weeks, we commonly use 48-well plates for tick cells because they accommodate a greater volume of medium per surface area than do 96 well plates, which reduces the need for feeding plate cultures. Tick cell culture plates are fed once 2 weeks after seeding.

3.3. Rationale of a dual host cell selection system

Due to the obligate intracellular nature of the *Anaplasmataceae*, a saturating mutant library is probably not achievable. However, we have found that *Ap* differentially express their genome depending on whether they reside in human or tick cells, with hypothetical genes expressed in greater numbers in tick cells. There also is a core set of genes, many encoding metabolic enzymes, expressed equally in both host types (Nelson et al., 2008). Genes absolutely required for intracellular survival are essential for *Ap* viability, and cannot be disrupted, but those only required for growth in one of the host cell types can be knocked-out without affecting replication in the other cell line. We have previously generated an *Ap* mutant with a transposon insertion in an *o*-methyltransferase gene that is required for infection of tick cells only, and displays wild-type growth kinetics in the human promyelocyte cell line HL-60, validating this approach (Oliva Chávez et al., 2015).

4. Constructs and their features

4.1. Transposon optimization

Himar1 transposition efficiency is negatively correlated with transposon size, such that every 1-kb increase in transposon size results in a 38% decrease (Lampe et al., 1998). To keep the transposon under 2 kb in size, the fluorescent reporter and spectinomycin resistance genes (*aadA*) were driven by a single promoter via translational coupling. Translational coupling utilizes a small intervening sequence that ensures that both proteins are transcribed on the same RNA strand and produced with similar stoichiometry (Tian and Salis, 2015). Therefore, we originally designed two plasmids that separately encoded the transposase and the transposon (Felsheim et al., 2006), but have since then combined both functions on a single *cis* construct (Munderloh et al., 2012). We hypothesized that the chances of a bacterium incorporating a single plasmid were much greater than the chances of a bacterium receiving both the transposon and the transposase plasmids, offsetting the reduction of transformation efficiency due to the larger construct. The codon usage of some biomarkers and resistance proteins differ greatly from that of *Ap*. To optimize the expression of these proteins we routinely utilize synthetic versions of fluorescent proteins and resistance markers that employ the codon usage patterns of *Bacillus subtilis* (purchased from DNA2.0 Inc. http://www.dna20.com/). We included the *lac* operator upstream of the HIMAR1 transposase sequence to reduce expression in *E. coli* during plasmid production. Once within *Ap*, the *lac* operator no longer functions, and expression can proceed. This is not a crucial feature of this construct, but it improves plasmid yield and fidelity.

4.2. Promoters

For our research, we have primarily used the well-characterized *A. marginale tr* promoter, which is homologous to the strong *Ap tr1* promoter. Both function in mammalian as well as in tick cells to drive expression of genes in the *msp2* cassette as a polycistronic message that is subsequently cleaved into individual components (Barbet et al., 2005). This is the site wherefrom variants of a major surface protein, MSP2, are transcribed, which is thought to underlie the organism's capacity for immune evasion (Futse et al., 2009). There is evidence that MSP2 variants also mediate invasion of different host cells (Chávez et al., 2012), demonstrating that the mechanism is active in both mammalian and tick host environments. The *tr* promoter was functionally optimized (Felsheim et al., 2006) and subsequently shown to drive strong and consistent expression of fluorescent and selectable markers in *Ap*, *Ehrlichia muris eauclairensis*, and *E. chaffeensis* (Cheng et al., 2013; Felsheim et al., 2006; Lynn et al., 2015; Pritt et al., 2017) For reasons that remain unanswered, we have never been able to clone an optimized, functional *tr1* promoter. In the future, it would be useful to develop a set of well-characterized promoters and associated regulatory elements, including those that can provide inducible or tissue-specific gene expression.

4.3. Selectable markers - antibiotics

When working with pathogenic bacteria, the choice of a selectable marker must take into consideration which antibiotics are used for treatment of the illness they cause, and antibiotics of therapeutic value must be avoided for selection. Fortunately, antibiotics that are not effective *in vivo* for various reasons such as inability to penetrate into appropriate cellular or tissue compartments, may well be suitable for in vitro selection. One such antibiotic that is only rarely used, and never for treatment of any rickettsial illness, is spectinomycin. It is able to penetrate into eukaryotic cells, and thus affects bacteria residing intracellularly. The gene encoding spectinomycin resistance, *aadA*, also imparts resistance against streptomycin. Dual selection can alleviate problems due to single-point mutations in *rpsE* encoding the Sr protein of the 30 s RNA, which can cause non-specific resistance to spectinomycin by changing ribosome structure.

4.4. Non-antibiotic selection

Non-antibiotic selection has been used to create field crops that can be grown in the presence of herbicides, to improve crop yields and avoid inclusion of weeds in the harvested product. Phosphinothricin (PPT), also known as Glufosinate and marketed as the herbicide Basta by Beyer, is useful for selection of transformed plants and bacteria that express resistance conferred by the *bar* gene (Herrero et al., 1990). *Bar* encodes PPT N-acetyltransferase that inactivates PPT through acetylation. It was discovered in *Streptomyces hygroscopicus* that also produces bialaphos (*bar*=bialaphos resistance), a tripeptide that when metabolized releases PPT, which acts as an analogue of glutamate, and competitively inhibits glutamine synthetase (Hoerlein, 1994; Thompson et al., 1987). Glutamine synthetase (GS) plays a central role in the regulation of eukaryotic and prokaryotic nitrogen metabolism. In susceptible organisms such as plants and bacteria, PPT causes cytosolic accumulation of ammonia and depletion of glutamine, which effectively results in killing intracellular bacteria without adversely affecting mammalian host cells. RPMI1640 cell culture medium for propagation of many human and animal cell lines does not provide sufficient glutamate or glutamine to offset the effect of PPT, so this selection system works well with them. PPT is able to reduce de number of HL-60 cells that are infected with *Ap* in a concentration dependent manner (Fig. 1). However, tick cells are grown in medium that supplies large amounts of glutamate, rendering PPT selection inoperable. To test if PPT could be used as an effective selection marker, we transformed *Ap* with a plasmid
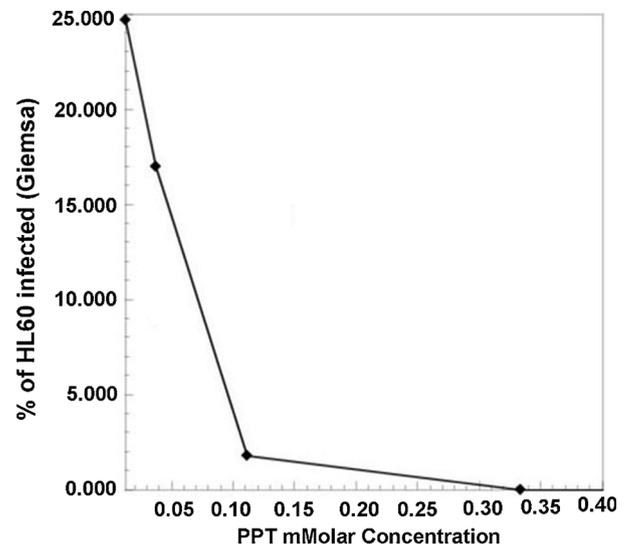

Fig. 1. Sensitivity of *A. phagocytophilum* wild-type bacteria grown in HL-60 cells to concentrations of phosphinothricin (PPT).
HL-60 cells infected with wild-type *A. phagocytophilum* were exposed to increasing concentrations of phosphinothricin (PPT). The number of infected cells was assessed through light microscopy after Giemsa-staining. A concentration of 100 mM PPT was subsequently chosen for selection.

containing the *bar* gene in replacement of the *aadA* gene used in (Felsheim et al., 2006). PPT-resistant *Ap* were generated with an efficiency equivalent to spectinomycin-resistant *Ap* in the presence of 100 mM PPT added the day following electroporation. Note that for transformation to generate PPT-resistant *Ap*, we used the original two-plasmid configuration where the transposon and the transposase are encoded on two separate plasmids that are added in equal amounts (1 μg each) to the bacteria in electroporation buffer, i.e., 300 mM sucrose (Felsheim et al., 2006). In future applications, these could also be combined into a single construct. Multiple selection mechanisms facilitate retrieval of mutants in secondary rounds of selection based on additional markers, e.g., when it is desired to recover mutant bacteria in which gene function has been restored with a functional copy of the originally disrupted gene, or when dual or triple mutants are sought.

4.5. Discovery of an effector

Random mutagenesis followed by phenotype assessment, identification of insertion site, and analysis of disrupted pathways provides an efficient mean to discover the function of hypothetical genes. This is a particularly valuable approach for bacteria the genomes of which encode a large proportion of hypothetical genes. Despite continuous efforts to improve the reliability of bioinformatics software for prediction of genes encoding bacterial effectors (Lockwood et al., 2011; Meyer et al., 2013), this remains difficult. We hypothesized that himar1 transposon mutants with insertions in genes required for infection of mammalian cells could be recovered in tick cell culture. To identify candidate mutants, we screened for impaired ability to efficiently infect and replicate in human HL-60 cells. Here, we describe the generation and characterization of an *Ap* mutant with an insertion in a gene that encodes a putative T4SS effector previously identified in infected HL-60 cell nuclei by mass-spectrometry (Sinclair et al., 2015). We show that the protein is translocated into the cytoplasms of infected cells, where it accumulates over time. This protein is necessary for *Ap* survival within HL-60 cells but not for infection of ISE6 tick cells, or hamsters. Accordingly, mutation of *aph_0906* using random transposition (Felsheim et al., 2006) disrupted the ability of *Ap* to replicate in HL-60 cells. Bioinformatic analyses also identified the presence of a putative Nuclear Localization Signal (NLS) and several protein-, DNA- and RNA-

binding sites, which are conserved in APH_0906 homologs found in several *Ap* strains despite divergence in their protein sequence.

5. Materials and methods

5.1. Culture, transformation, recovery

The human anaplasmosis isolate HGE2 was initially obtained from patient blood cultured with the human promyelocyte line, HL-60 (Goodman et al., 1996), and subsequently propagated in the *I. scapularis* tick cell line ISE6 (Munderloh et al., 1999). Bacteria were purified from $\sim 10^7$ mechanically disrupted tick cells, washed twice in 270 mM sucrose, and incubated in 50 μl sucrose with 1 μg of each transposon-(containing the *gfp_uv* and *aadA* genes, pHIMAR1-UV-SS) and *himar1* transposase-encoding plasmids for 15 min on ice before electroporation in a 0.2 mm gap cuvette at 1.8 kV, 400 Ω and 25 μF using a GenePulserII (Biorad) (Felsheim et al., 2006). Bacteria were immediately recovered in 0.5 ml culture medium with 20% FBS, and spread over a confluent layer of ISE6 cells. After 30-min incubation at 34 °C, 5 ml complete medium was added, and spectinomycin plus streptomycin (100 μg/ml each) were included for selection of transformants the next day. The culture was monitored for GFP-expressing bacteria using a Nikon Diaphot inverted microscope (Nikon, New York) fitted for epifluorescence detection, and fed twice weekly with medium containing antibiotics for selection. Intracellular inclusions of transformants were first seen 4 weeks after electroporation, and transformants continued to replicate similar to wild-type.

5.2. Determination of insertion site

Southern blot analysis was used to determine the number of insertion sites. DNA from the mutant (designated ΔAPH_0906) and wild-type HGE2 bacteria grown in ISE6 cells was purified using the Puregene Core Kit A (Qiagen, Maryland) followed by phenol/chloroform extraction to remove remaining proteins. DNA (100 ηg), from each sample, was digested with *Bgl*II, *Hind*III and *Eco*RI and electrophoresed in 1% agarose gels at 30 V overnight, and then blotted onto membranes and probed as described (Felsheim et al., 2006). Digoxigenin-labeled probes to detect *gfp_uv* were generated with the PCR DIG Probe Synthesis kit (Roche, Indiana), and the pHIMAR1-UV-SS construct was used as positive control.

The location of the transposon in the APH_0906 coding region was determined by rescue cloning of *Bgl*II digested DNA into the pMOD plasmid which was electroporated into ElectroMAX DH5α cells (Invitrogen, New York). ElectroMAX DH5α cells were selected on YT plates with 50 μg/ml of spectinomycin and streptomycin. DNA from one colony was sequenced at the BioMedical Genomics Center (University of Minnesota).

5.3. Growth characteristics of ΔAPH_0906

HL-60, RF/6 A and ISE6 cells were routinely maintained as described (Goodman et al., 1996; Munderloh et al., 2004, 1999). Growth of the mutant in HL-60, RF/6 A and ISE6 cells was determined from two replicate cultures inoculated with bacteria purified from ISE6 cells (Oliva Chávez et al., 2015). Bacteria were resuspended in supplemented RPMI1640 (HL-60) or L15C300 medium (RF/6 A and ISE6) and inoculated into 12.5-cm^2 flasks containing 3.6×10^5 uninfected HL-60 cells, or confluent layers of RF/6 A or ISE6 cells. Cultures were monitored weekly by epifluorescence microscopy of live cultures and by bright-field microscopy of fixed and Giemsa-stained preparations. qPCR of the single copy gene *msp5* was used to determine bacterial numbers (Oliva Chávez et al., 2015).

5.4. Infection of hamsters with ΔAPH_0906

To test the ability of ΔAPH_0906 to infect mammals, nine 2-week old hamsters were injected i.p. with 500 μl of infected ISE6 cells. After 7 days, heart blood from two euthanized hamsters was cultured with HL-60 and ISE6 cells. DNA was extracted from the remaining blood. Inoculated ISE6 and HL-60 cultures were monitored bi-weekly by epifluorescence microscopy as above. Remaining hamsters were euthanized 21 days p.i., and DNA was extracted from blood and tested for presence of *Ap*16S rDNA using nested primer pairs EE1-EE2 and EE3-EE4 (Yang et al., 2016).

5.5. Relative gene expression of Aph_0906

Wild-type HGE2 *Aph_0906* expression was compared in ISE6 and HL-60 cells incubated under standard conditions for 4, 24, 48, or 72 h. Total RNA was extracted from whole infected cells using the Absolutely RNA Miniprep Kit (Agilent, California), and remaining DNA was eliminated by two treatments of the eluate with TURBO DNAse (Ambion, New York). Gene expression was normalized against expression of *RNA polymerase subunit B* (*rpoB*) and *major surface protein 5* (*msp5*) genes. *rpoB* is a housekeeping gene and part of the DNA-directed RNA polymerase pathway necessary for transcription, and *msp5* is a single copy gene that is expressed in both cell lines with no significant difference in expression (Nelson et al., 2008). qRT-PCR reactions were carried out using the primers described in Table 2 with Brilliant II QRT-PCR SYBR Green Low ROX Master Mix (Agilent, California). Reaction conditions were one cycle at 50 °C for 30 min, one denaturing cycle at 95 °C for 10 min, 40 cycles that consisted of 30 s at 95 °C, 1 min at 50 °C, and 1 min at 72 °C, and a final cycle of 1 min at 95 °C and 30 s at 50 °C.

Table 2
Primers used in the study.

Primer name	Primer sequence	Target	Use	Restriction site	Piece size (bp)	Reference
aph_0906 fw	AGCTCATATGCACAACTATG	APH_0906	qRT-PCR	N/A	247	This paper
aph_0906 rev	AAACGGACACTCTCTATGTT	APH_0906	qRT-PCR	N/A	247	This paper
rpoB fw	CTTTATCCTGCTTTAGAACAACATC	rpoB	qRT-PCR	N/A	286	Oliva Chávez et al (2015)
rpoB rev	GGTCCGTATGGTCTGGTTACTC	rpoB	qRT-PCR	N/A	286	Oliva Chávez et al (2015)
msp5 F1	TGACACTGTGGTTGAACAAGC	msp5	qPCR and qRT-PCR	N/A	126	Oliva Chávez et al (2015)
msp5 R1	GAAGAAAAGCCGAACATAAGC	msp5	qPCR and qRT-PCR	N/A	126	Oliva Chávez et al (2015)
APH_0906 fw1	ATGGTAGCATATGATGACTCTGCTGCTTAAGCCAAAC	APH_0906	Recombinant protein	NdeI	2268	This paper
APH_0906 rv1	GTGATGCCTCGAGATCGATCAGAGTGTCACCGAGCAT	APH_0906	Recombinant protein	XhoI	2268	This paper
APH_0906 fw2	GTGCGATCCATGGAAGAAGATGGTACCGCGT	APH_0906	Recombinant protein	NcoI	2462	This paper
APH_0906 rv2	ATTGCTTAGCTCGAGATGCTGCTGCTGTGATACG	APH_0906	Recombinant protein	XhoI	2462	This paper
T7 promoter	TAATACGACTCACTATAGGG	pET28 vector	Sequencing	N/A	N/A	Novagen
T7 terminator	GCTAGTTATTGCTCAGCGG	pET28 vector	Sequencing	N/A	N/A	Novagen

Ct values were established during amplification and the dissociation curve was determined during the final denaturation cycle. The relative expression of *aph_0906* was determined from two replicates, using the $2^{-\Delta\Delta ct}$ method.

5.6. Production of recombinant APH_0906, mouse immunization

To facilitate localization of protein, we produced recombinant wt-APH_0906 protein for antibody production. Due to the size of the *APH_0906* locus (4587 bp), the two halves of the ORF were cloned into the pET29a expression vector (Novagen, Germany). The portion between nucleotides 965395–967663 (r1APH_0906) was amplified using primers APH_0906 fw1 and APH_0906 rv1, and the second half (r2 APH_0906), located between nucleotides 967516–969978 was amplified using primers APH_0906 fw2 and APH_0906 rv2 (Table 2). PCR conditions were one denaturing cycle at 94 °C for 3 min, 10 cycles with a denaturing step at 94 °C for 1 min, annealing at 48 °C for 1 min, and extension at 72 °C for 2 min, followed by 20 additional cycles with a denaturing step at 94 °C for 1 min, 60 °C for 1 min for annealing, and extension at 72 °C for 2 min, and a final extension step of 7 min at 72 °C. Amplified products were digested with *Xho*I and *Nde*I (r1APH_0906) and *Xho*I and *Nco*I (r2 APH_0906), and ligated overnight into pET29a at 15 °C. Plasmids were cloned into One Shot® TOP10 competent cells (Invitrogen, Grand Island, NY), purified using the High pure plasmid isolation kit (Roche, Indianapolis, IN), and sequenced at the Biomedical Genomics Center (University of Minnesota). Plasmids were transfected into BL21(D3) *E. coli* (New England Biolabs, Massachusetts) and induced with 200 μM IPTG in 100 ml of Superior Broth (AthenaES, Baltimore, Maryland) (final concentration) at 37 °C overnight with constant shaking. Recombinant r1APH_0906 and r2 APH_0906 were purified using Ni-NTA Fast Start Kit columns (Qiagen, Germantown, Maryland), and dialyzed against TBS in 3 ml Slide-A-Lyzer Dialysis Cassettes with a 10-kDa molecular weight cut-off (Thermo Scientific, Illinois). Protein concentrations were measured using the BCA protein assay kit (Pierce, Illinois). The correct molecular weight of recombinant proteins was verified by electrophoresis on a 4–15% Mini protean TGX gel (Biorad, California) stained with Coomassie blue.

Three 6–8 weeks old C57BL/6 J female mice (Jackson Laboratories, Maine) were injected subcutaneously at the base of the tail with 100 μg of each recombinant protein emulsified in TiterMax Research adjuvant (CytRx Co., Georgia), and boosted 14 days and 24 days later. Antiserum was collected 10 days after the third booster from heart blood after CO_2 euthanasia, and serum from naive mice was used as a control.

5.7. APH_0906 localization

Infected HL-60 cells (2.7×10^4) were inoculated into five 25-cm^2 flasks containing 2×10^5 uninfected HL-60 cells in supplemented RPMI1640. Cultures were incubated at 37 °C and the contents of one flask were processed for detection of APH_0906 each day for 5 days as follows. Cells were collected at 2000 x g for 10 min, fixed in 4% paraformaldehyde in PBS overnight at 4 °C, and then washed three times with 1% BSA in PBS for 5 min. Cells were permeabilized for 10 min in 1% BSA in PBS with 0.1% saponin and 0.1% sodium azide at room temperature. To detect APH_0906 and *Ap*, cells were incubated with anti-r1APH0906 (1:250) and polyclonal dog anti-*Ap* antibodies (1:500), respectively, for 2 h at room temperature and then labeled with Cy3-labeled anti-mouse or FITC-labeled anti-dog IgG (each at 1:1000) for 1 h at room temperature. Labeled samples were washed, centrifuged, and resuspended in 2 ml 1% BSA in PBS, and 10 μl volumes spotted onto Silane-prep™ slides (Sigma-Aldrich, Missouri). VectaShield mounting medium with DAPI (Vector laboratories, California) was added to label host cells nuclei. Samples were viewed on an Olympus BX61 confocal microscope (Olympus America, Pennsylvania) equipped with a DSU-D2 confocal disk-scanning unit, and images were acquired with a Photometrics QuantEM:512SC EMCCD camera (Photometrics, Arizona)

or a QFire color camera (Qimaging, California). Metamorph (Molecular Devices, California) and ImageJ (US National Institutes of Health) were used to capture and compile z-projections, and Photoshop (Adobe Systems, California) was used for cropping and adjustment of brightness/contrast.

In an effort to localize APH_0906 at specific times during bacterial replication, we synchronized HL-60 cell infection with wild-type *Ap* and imaged samples taken 1 day, 3 days, and 5 days p.i. as described above. Bacteria were purified from a fully infected 25-cm^2 flask using mechanical disruption and filtration (Oliva Chávez et al., 2015), and combined with 2.5×10^5 HL-60 cells in 200 μl of supplemented RPMI1640 medium. APH_0906 was localized within infected cells using mono-specific r2-APH0906 antibodies and imaged as above.

5.8. Bioinformatics-based comparison of APH_0906 homologs

Secondary and tertiary structures of APH_0906 were modeled using i-TASSER (Yang et al. 2015). The predicted gene ontology (GO) was inferred from the most similar protein with a crystal structure deposited into the Protein Data Bank (PDB) based on the amino acid alignment generated using LOMETS (Local Meta-Threading-Server) (Wu and Zhang, 2007). Because of restrictions on the size of the protein, two separate models for each half of the protein were generated.

The protein sequences of the APH_0906 homologs from strains Webster (APHWEB_1100; Accession # KJV60642), HGE1 (HGE1_03857; Accession # EOA61157), HGE2 (APHGE2_1212; Accession # KJV82470), ApWI1 (APHWI1_0415; Accession # KJV85064), Annie (OTSANNIE_1184; Accession # KJV98448), CR1007 (APHCR_0401; Accession # KJZ99081), JM (WSQ_04155; Accession # AGR80798), Dog2 (YYY_04145; Accession # AGR82050), MRK (O997_04170; Accession # KDB56310), Norway variant 2 (P029_03620; ANC34432), ApMUC09 (APHMUC_0611; Accession # KJV63589), CRT35 (P030_05350; KDB57323), CRT38 (CRT38_03747; EOA62348), ApNP (APHNP_0408; Accession # KJV68008), and NCH-1 (EPHNCH_1234; Accession # KJV63015) were downloaded from GenBank (https://www.ncbi.nlm.nih.gov/protein/). Sequences were aligned using MUSCLE in Geneious R10 (Biomatters LTD, Auckland, New Zealand), generating a similarity matrix with the total number of differences in each sequence. This alignment was then used to generate phylogenetic trees using the Neighbor-Joining and UPGMA in MEGA7 (Kumar et al., 2016). The positions of protein, DNA, and RNA binding residues within the amino acid sequence of each homolog were predicted using DisoRDPbind (Peng and Kurgan, 2015), and Nuclear Localization Signals (NLSs) were predicted using NLSmapper (Kosugi et al., 2009) and NLStradamus (Nguyen Ba et al., 2009). These features were annotated for each sequence using Geneious R10. Putative Domains were investigated with SMART (Letunic et al., 2015).

5.9. Ethics statement

The use of animals in this study was approved by The Institutional Animal Care and Use Committee (IACUC) of the University of Minnesota. All animal experiments were carried out following the guidelines of the National Institutes of Health guide for the care and use of laboratory animals.

6. Results

6.1. Disruption of aph_0906 affects growth of Ap in HL-60 cells

Random transposon mutagenesis of *Ap* (Felsheim et al., 2006) has proven valuable for analysis of genes required for mammalian pathogenesis (Chen et al., 2012) and invasion of tick vector cells (Oliva Chávez et al., 2015). Here, we describe an *Ap* HGE2 transposon mutant that was recovered and propagated in an *I. scapularis* cell line (ISE6). Southern blot analysis identified one band in *Bgl*III, *Eco*RI, and *Hind*III
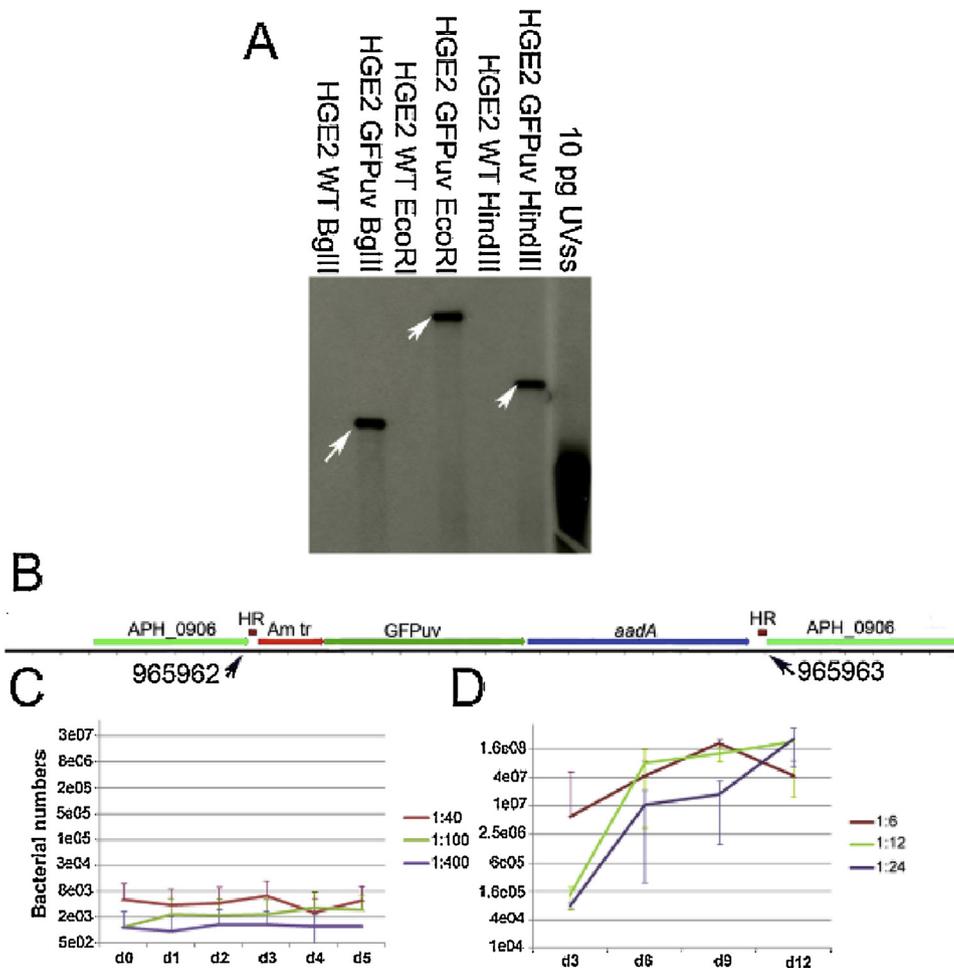
digested samples (Fig. 2A), suggesting that a single insertion event had occurred. Thus one *E. coli* clone was sequenced. The sequencing result demonstrated an insertion event into *aph_0906* (Gene ID: 3930,051), a gene encoding a hypothetical protein, at nucleotide positions 965962–965963 (Fig. 2B) of the HZ genome (corresponding to positions 1161199–1161200 in the HGE2 genome; Locus tag LAOE01000001.1). The mutant was designated ΔAPH_0906.

Whole genome-tilling array gene expression analysis has shown that *aph_0906* transcription is highly upregulated during infection of HL-60 but not ISE6 cells (Nelson et al., 2008). Indeed, microscopy of HL-60 cells inoculated with ΔAPH_0906 infected ISE6 cells or purified bacteria indicated that the bacteria were unable to form morulae and replicate in HL-60 cells, prompting more detailed analyses to determine the step at which infection by the mutant failed. ΔAPH_0906 persisted in HL-60 cells for up to 5 days post-inoculation without an increase in bacterial numbers (Fig. 2C), while replication of ΔAPH_0906 in ISE6 cells was not affected (Fig. 2D). These results indicate that although APH_0906 is necessary for replication within HL-60 cells, this gene is unessential for ISE6 infection. Genes that are essential for infection of the mammalian host but not for the infection of ticks have been reported in *E. chaffeensis* (Cheng et al., 2015). Four different mutants, generated by random mutagenesis, were impaired in their ability to infect deer and dogs, however they were detected in *Amblyomma americanum* ticks (Cheng et al., 2015). This indicates that the differential requirement of specific genes for infection of the tick vector and the mammalian host may be a mechanism shared between members of the *Anaplasmataceae* family. This could be partially explained by the differential gene expression between tick and mammalian cells (Nelson et al., 2008).

6.2. ΔAPH_0906 development in RF/6 A cells is impaired, but it is able to infect hamsters

Since ΔAPH_0906 was unable to productively infect HL-60 cells, we tested its capacity to replicate in a non-human primate endothelial cell line, RF/6 A, which supports the growth of wild-type bacteria, and since microvascular endothelium has been suggested to be a target of infection (Herron et al., 2005). Bacteria readily adhered to RF/6 A cells, but their number appeared to decrease with time as fewer bacteria were detected by day 6, and on day 14, only a few small morulae remained visible in Giemsa-stained cells (Fig. 3B).

We then tested if ΔAPH_0906 was able to infect rodents. Amplification of an 867 bp fragment of *Ap* 16 s rDNA from blood by nested PCR demonstrated that 7 of 9 hamsters injected with ΔAPH_0906 from ISE6 cultures became infected (Fig. 3 A), and 5 of them (lanes 3–9) remained infected for 21 days. Blood samples from hamsters injected with uninfected ISE6 cells did not show amplification of any product (negative control, lanes A). These results suggest the ability of ΔAPH_0906 to infect mammals, although the target cell remains to be identified. We did not confirm by sequence analysis that bacteria within the hamsters had not lost their inserts although the mutants reisolated into ISE6 cells from one hamster retained green fluorescence and spectinomycin-resistance, indicating presence of the transposon. Likewise, it remains to be determined whether there is a defect in the growth of ΔAPH_090 in rodents when compared to wild-type bacteria. Overall, these results suggest that while APH_0906 expression may be essential for replication in HL-60 and RF/6 A cells, the lack of this protein does not abolish infection of rodents.
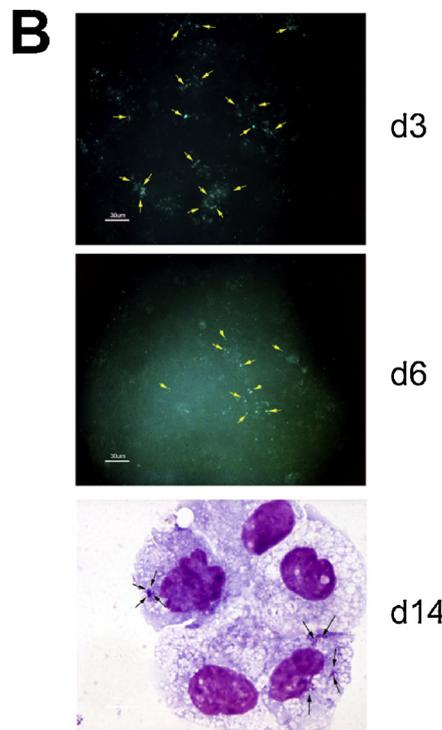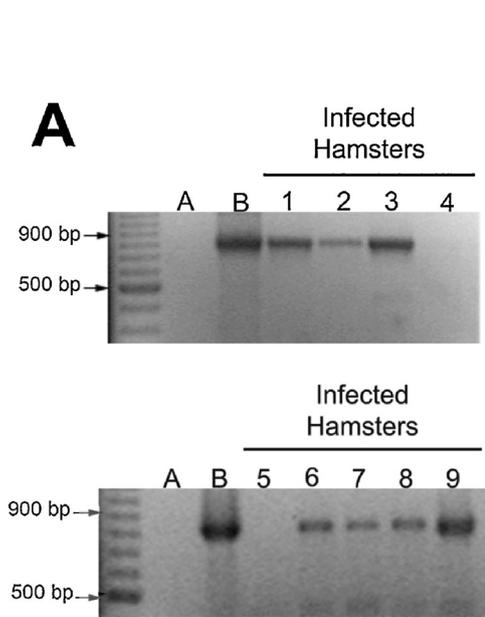
Fig. 3. ΔAPH_0906 infects hamsters during *in vivo* challenge but it is not able to replicate in RF/6 A cells *in vitro*.

Nine hamsters were challenge with 500 μl of ISE6 cells infected with ΔAPH_0906 bacteria by intraperitoneal (i.p.) injection. Two blood samples were taken 7 days days post-inoculation (p.i.) and the remaining 7 samples were taken at 21 days. DNA was purified from blood samples and nested PCR was used to confirm infection. The two samples taken at day 7 (Lanes 1 and 2) were positive and 5 out of 7 samples were positive at day 21 (Lanes 3–9). DNA from infected cells was used as positive control and the negative control consisted of mice injected with uninfected ISE6 cells. B) RF/6 A cells were inoculated with cell free ΔAPH_0906 bacteria. Infections were observed by fluorescence microscopy at day 3 and day 6. Bacteria (pointed by yellow arrows) were observed as green fluorescence associated with cells. This fluorescence appeared to decrease as time passed. Giemsa stains from infected RF/6 A at day 14 post-infection (p.i) show very small morulae, suggesting that the bacteria were not able to replicate within the infected cells.

6.3. aph_0906 expression in HL-60 increases over time

The change in expression of *aph_0906* in HL-60 at 4, 24, 48, and 72 h was measured by qRT-PCR, using *rpoB* and *msp5* as normalizer genes, respectively. Expression increased as infection in HL-60 cells progressed, starting at 0.005 and 0.001 at 4 h, and growing to 0.001 and 0.01 by 24 h, 0.012 and 0.03 by 48 h, and reaching 0.15 and 0.249 by 72 h (Fig. 4). These numbers represent a 10-, 30-, and 249- fold upregulation of the gene by 24, 48, and 72 h, respectively, when compared to the expression at 4 h and normalized by *msp5* expression. *Ap* has a biphasic life cycle comprising two functional forms. The invasive, or dense core form, binds to host cells and the reticulated form replicates inside a membrane bound vacuole (Troese and Carlyon, 2009). Expression of *aph_0906* was lowest at 4 h pi, coinciding with
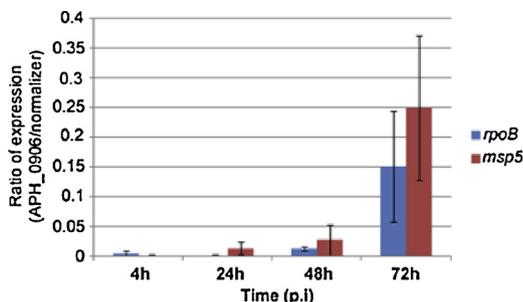

Fig. 4. APH_0906 mRNA expression within ISE6 and HL-60 cells shows an increase in transcription levels in HL-60 cells.

The ratio of expression of the gene encoding the hypothetical protein APH_0906 during infection of HL-60 cells was measured by qRT-PCR at 4, 24, 48, and 72 h p.i. Expression of the gene increased as the infection progressed when normalized against both normalizing genes, *rpoB* (blue bars) and *msp5* (red bars). The ratio of expression was calculated using one delta change of the Ct values ($2^{\Delta target - normalizer}$). B) The fold change in mRNA transcription of APH_0906 between ISE6 cells and HL-60 cells was measured at same time points described before. The fold change was calculated using the $2^{-\Delta\Delta ct}$ method. As described for the ratio of expression, the transcript levels of APH_0906 increased over time with up-regulation of the gene by 48 h and 72 h of infection when normalized by both genes, *rpoB* (blue bars) and *msp5* (red bars).

internalization of *Ap*, and increased over the course of 72 h, when bacteria had changed into the reticulate form undergoing intracellular multiplication (Troese and Carlyon, 2009). These results suggest that the expression of *aph_0906* facilitates intracellular replication but not invasion, which may explain why we were able to detect bacterial DNA in HL-60 cells for up to 5 days although bacterial numbers did not increase (Fig. 2C). A similar increase in the expression of an *Ap* effector during intracellular infection was reported for APH_1387, which is a protein associated with the vacuolar membrane. APH_1387 expression increased from 8 h p.i. and reached its maximum by 48 h p.i. (Huang et al., 2010).

6.4. APH_0906 is translocated into the cytoplasm of infected cells

To determine the localization of APH_0906 at different time points during infection of HL-60 cells, we performed Immunofluorescence Assays (IFAs) and confocal microscopy, using antibodies against the recombinant versions of APH_0906, r1-APH0906 and r2-APH0906. Wild-type bacteria were added to uninfected HL-60 cell cultures, and samples were taken on days 1, 3, and 5 p.i. APH_0906 protein was detected using polyclonal antibodies against r1-APH_0906 or r2-APH_0906. Confocal microscopy was used to visualize the location of the protein within infected cells. On day 1 p.i., most APH_0906 co-localized with the bacteria as demonstrated by the yellow signal produced by co-localization of Cy3 (red) anti-APH_0906 and FITC (green) anti-*Ap* labels. A small amount of red signal was observed in the cytoplasm of the host cell in close proximity to the bacteria (Fig. 5; Videos S1).

On day 3 p.i., APH_0906 was mostly observed in the proximity of the morulae and in some cases randomly dispersed in the cytoplasm (Fig. 5; Videos S2). In heavily infected cells harboring several morulae, some APH_0906 protein associated with the DAPI (blue) signal from the host cell nucleus (Fig. 5; Video S3), although this association may be an artifact. By day 5 p.i., the protein appeared as aggregates that accumulated in the cytoplasm of infected cells surrounding large morula (Fig. 5; Videos S3). APH_0906 became more abundant as the infection progressed confirming our expression data and the results of the tiling array (Nelson et al., 2008) (Fig. 5; Video S1-3). Sinclair et al (Sinclair
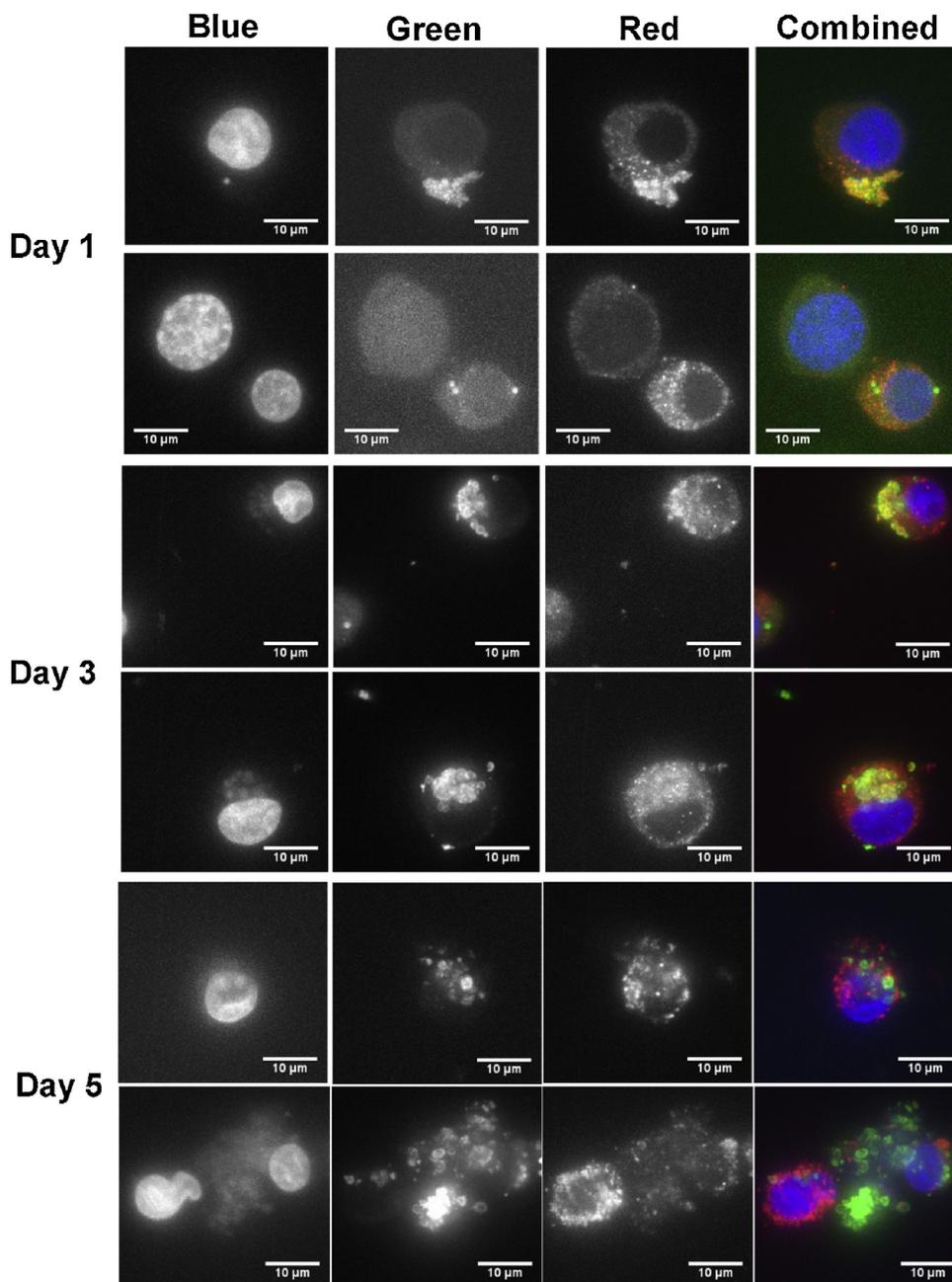
Fig. 5. Subcellular localization of APH_0906 during infection of HL-60 cells.

The subcellular localization of APH_0906 was investigated with Immuno Fluorescence Assays (IFAs) of infected HL-60 cells at 1, 3, and 5 days p.i. The bacteria were labeled with dog serum against *A. phagocytophilum* detected with FITC anti-dog antibodies (green signal). APH_0906 was labeled using mouse serum raised against recombinant versions of APH_0906 and detected with Cy3-labeled anti-mouse antibodies (red signal). The nucleus of the cells was labeled with DAPI (blue signal). Localization of the protein at day 1 was mostly associated with the bacteria and as infection progressed the protein was translocated into the cytoplasm of the cells by day 3 and 5. A 10 μm size bar is included in the pictures for comparison.

et al., 2015) detected APH_0906 in nuclear preparations from infected cells using proteomics. We did not conclusively observe APH_0906 in the nucleus of infected cells. These discrepancies could be due to cytoplasmic contamination in the nuclear preparations used (Sinclair et al., 2015) or that we missed the specific time point during our observations. According to our observations, APH_0906 can be observed co-localizing with morulae containing bacteria and being translocated into the cytoplasm at day 1 and day 3, but as infection progresses (day 5) the protein localizes mostly to the cytoplasm of infected cells (Fig. 5). This suggests that APH_0906 might likely complete its function in the cytoplasm of infected cells.

6.5. APH_0906 has no predicted domains

We used bioinformatic approaches to obtain insights into the potential function of APH_0906. BLAST analysis of the protein provided no information on potential domains and motifs present in the protein. Furthermore, no homologs of the proteins were identified outside of the

Anaplasmataceae family and all hits represented proteins without known function, hence its hypothetical status. Likewise, SMART analysis of the APH_0906 protein sequence did not return any domain with significant value. The tertiary structure of the protein was inferred with i-TASSER to find proteins with known crystal structure that presented high sequence similarity to APH_0906. Comparison of the APH_0906 predicted protein sequence to proteins with known crystal structure retrieved three top models with > 0.8 TM-Score. The top score corresponded to Brr2 Helicase Region (PDB ID: 4F91; TM-Score: 0.892), which is an RNA helicase that is essential for spliceosome activation (Plaschka et al., 2017) and disassembly (Santos et al., 2012). The second top-score model belonged to a homolog of Brr2 in *Chaetomium thermophilum* (PDB ID: 5M59; TM-Score: 0.863) (Absmeier et al. 2017) and the third top-score model corresponded to the Brr2 homolog in *Saccharomyces cerevisiae* (PDB ID: 4BGD; TM-Score: 0.839) (Nguyen et al., 2013), strengthening the prediction. Functional prediction by Gene Ontology of the predicted models suggested that APH_0906 may have RNA helicase (GO:0034458 and GO:0004004; GO-Score: 0.35),
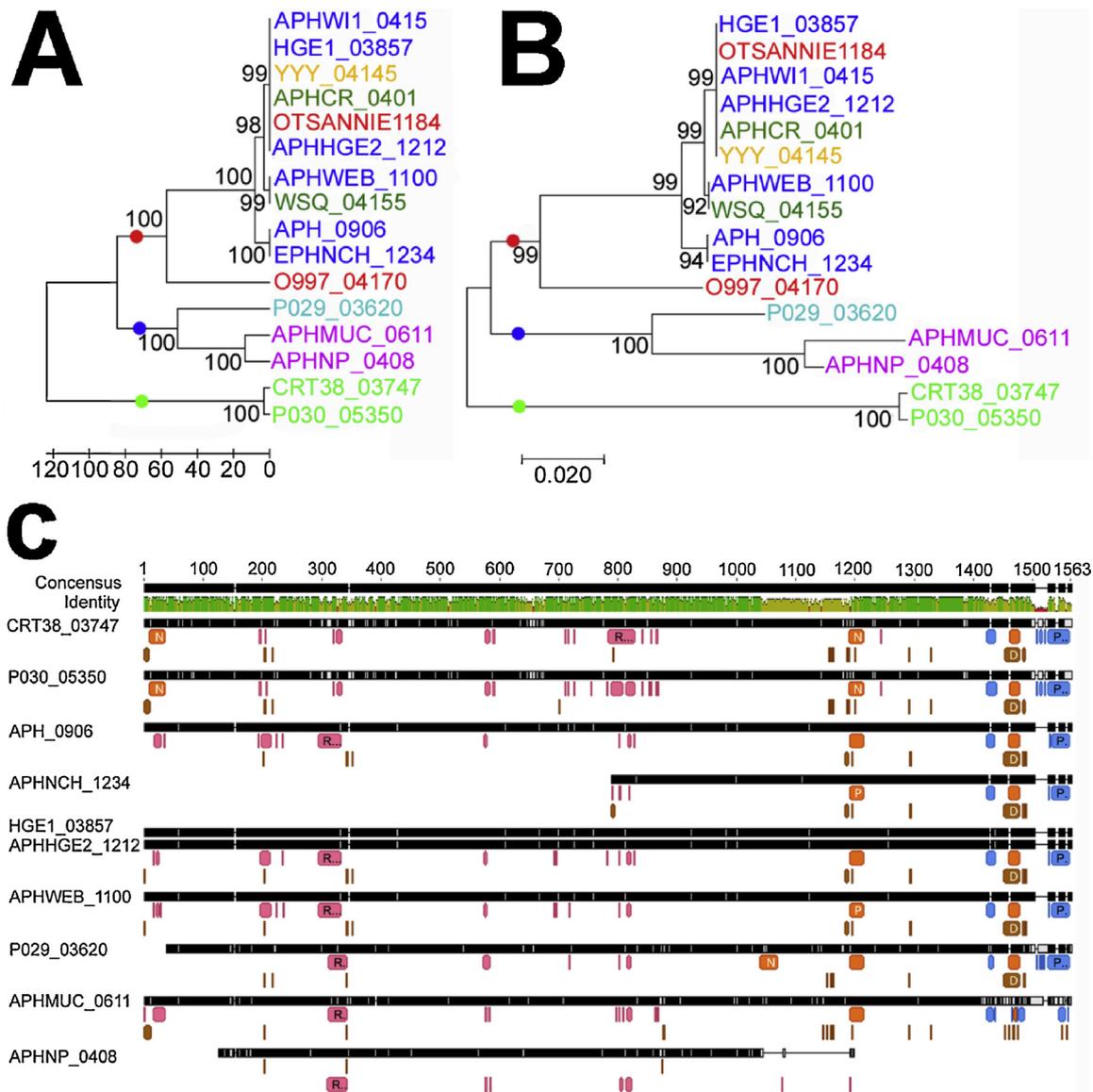
Fig. 6. Bioinformatic analysis of APH_0906 and its homologs.
Phylogenetic relation between homologs of APH_0906 from *A. phagocytophilum* strains isolated from different hosts analyzed with the UPMAG and B) Neighbor-Joining methods. Strains isolated from human hosts in the US are depicted in dark blue, strains isolated from horses in the US in red, strains isolated from rodents in the US in dark green, strains isolated from ticks in the US in light green, and a strain isolated from a dog in the US is shown in yellow. Strains isolated from dogs in Europe are shown in purple and a strain isolated from a sheep in Norway is shown in light blue. The boostrap values were inferred from 1000 replicates. Three different clusters were identified with dots of different colors at the base of the branches. The red dot identifies a cluster (Cluster 1) formed by APH_0906 homologs from strains isolated from vertebrates in the US. The second cluster (Cluster 2; blue dot) is composed by homologs from strains isolated from vertebrate hosts in Europe, and the last cluster (Cluster 3; green dot) is represented by homologs from strains isolated from ticks in the US. C) MUSCLE alignment of APH_0906 homologs from different clusters showing predicted characteristics within the amino acid sequences. RNA binding sites are represented by pink boxes under the amino acid residues. DNA binding sites are shown in brown and protein binding sites are shown in blue. Predicted Nuclear Localization (NLSs) are shown in orange. Binding sites were predicted with DisoRDPbind and NLSs with NLSmapper and NLStradamus. Image was generated with Geneious R10.

mRNA-binding (GO:0003729; GO-Score: 0.35) and ATP-binding (GO:005524; GO-Score: 0.41) activities. Interestingly, *Ap* infection of HL-60 cells differentiated into neutrophils with ATRA affects the expression of specific gene isoforms, including 9 genes encoding components of the spliceosome complex (Dumler et al., 2018). Brr2 is a key component of the spliceosome complex and is implicated in its activation, splicing catalysis and disassociation. Because Brr2 interacts with several other component of the spliceosome, authors have speculated that it may indirectly act in alternative splicing (as reviewed in (Absmeier et al., 2016)). Our bioinformatics analysis predicts similarities between APH_0906 and Brr2; however, whether or not APH_0906 binds to mRNA and can affect spliceosome assembly leading to changes

in ASEs expression needs to be functionally determined.

6.6. Phylogenetic distribution and amino acid differences correlate with strain host tropism but predicted binding sites are conserved between APH_0906 homologs

Host tropisms differences have been reported between *Ap* strains in the US, with a subset of strains able to infect humans, dogs, and horses (reviewed in (Dugat et al., 2015)). The phylogenetic clustering of AnkA, a known *Ap* effector protein, correlates with host species (Majazki et al., 2013; Scharf et al., 2011). We wanted to see if a similar phenomenon applied to other effectors. The amino acid sequence from twelve

Table 3
Nuclear Localization Signals (NLSs) predicted for the homologs of APH_0906.

		NLS Mapper		NLStradamus	
Protein	Host	NLS Sequence	Score	NLS Sequence	Cutoff
APH_0906	Human	KRHGRVLPTPMDPKVLQDLRSSNLLAA	4.8	TDGKKPSTTVPKKPPRPARGAK	0.6
EPHNCH_1234	Human	KRHGRVLPTPMDPKVLQDLRSSNLLAA	4.8	TDGKKPSTTVPKKPPRPARGAK	0.6
APHWEB_1100	Human	KRHGRVLPTPMDPKVLQDLRSSNLLAA	4.8	TDGKKPSTTVPKKPPRPARGAK	0.6
HGE1_03857	Human	KRHGRVLPTPMDPKVLQDLRSSNLLAA	4.8	TDGKKPSTTVPKKPPRPARGAK	0.6
OTSANNIE_1184	Human	KRHGRVLPTPMDPKVLQDLRSSNLLAA	4.8	TDGKKPSTTVPKKPPRPARGAK	0.6
O997_04170	Horse	KRHGRVLPTSMDPKVLQDLRSYNLLAA	4.8	KGTDGKKPSTTAPKKPPRSARGAK	0.6
P029_03620	Sheep	RGGYRNSKDVVEVIASGPDGLFTARPYLVKLRKGS RKRHGRVLPTPTDPEVLQDLRSSNLLAA	6.1 5.8	DGKKSSTTAPKKPPRTARGAK	0.6
CRT38_03747	Tick	PIKRHGSVLPTPMDPKVLQDLRSSNLLAA PSKRSTALLGSAIDFLLCRDQNSNPARQRI	5.2 4.9	GKKPSTTVHKKPPRPARGAK	0.6
P030_05350	Tick	PIKRHGSVLPTPMDPKVLQDLRSSNLLAA PSKRSTALLGSAIDFLLCRDQNSNPARQRI	5.2 4.9	GKKPSTTVHKKPPRPARGAK	0.6
APHNP_0408	Dog	None	N/A	None	N/A
APHMUC_0611	Dog	LKRHGRVLPTPMDPKALQDLISSNLLAA	4.8	PPKKPPRHA	0.6

APH_0906 homologs present in different *Ap* strains were downloaded from NCBI, aligned, and used for phylogenetic analysis. The number of amino acid differences between homologs ranged from 0 to 337 aa (Table S1). Two trees, showing identical groupings, were constructed using UPMAG (Fig. 6A) and Neighbor-Joining (Fig. 6B). APH_0906 homologs appeared to cluster according to host and continent of origin. Cluster 1 contained homologs present in US strains from humans, dog, rodents, and horses, whereas Cluster 2 comprised homologs from European sheep and dog strains, and Cluster 3 included homologs from US tick isolates (Fig. 6A and B). A similar grouping of human, dog, and horse strains into one cluster was reported for AnkA variants (Scharf et al., 2011). However, unlike AnkA, APH_0906 sequences of European dog strains clustered with a sheep strain of European origin and not dog strains from the US. Nevertheless, the European dog and the Norwegian sheep sequences in Cluster 2 are clearly divergent. Genomic differences between human pathogenic and non-human pathogenic strains have been reported. Human pathogenic strains presented higher homology and synteny with other human and dog isolates than with tick isolates from the US and ruminant isolates from Europe (Barbet et al., 2013). Interestingly, our phylogenetic analysis of APH_0906 showed a similar trend.

Due to the differences detected in the protein sequences of the different APH_0906 homologs from other strains, we decided to compare changes in putative binding sites. APH_0906 also possesses a potential Nuclear Localization Signal (NLS). Prediction of the DNA, RNA, and protein binding sites in the different homologs showed that binding sites are highly conserved in their position (Fig. 6C). Likewise, predicted NLSs were consistent in their position within most sequences with the exception of P029_03620 and the homologs from strains isolated from Camp Ripley ticks (CRT38_03747 and P030_05350) (Fig. 7C and Table 3), which were derived from engorged female ticks collected from white-tailed deer. It is likely that the CRT isolates are specific to deer in this region. There was an obvious trend in the distribution of the predicted binding sites within the homologs. Predicted RNA binding sites were mostly localized within the first 900 aa from the N-terminus of the protein, whereas the protein and DNA binding sites were located within the last 600 aa of the C-terminus and corresponded to half with the predicted NLSs (Fig. 6C). Only CRT38_03747 and P030_05350 possessed a predicted NLS within the N-terminus of the protein (Fig. 6C and Table 3). Whether these NLSs and binding domains are functional remains to be determined, but it is interesting that differences exist between human pathogenic strains and non-human pathogenic strains. One could speculate that these differences are due to adaptations acquired by human pathogenic strains (Table 3).

7. Conclusions

We have developed a system for the random mutagenesis of genes within members of the *Anaplasmataceae* family. Through our experience, we have improved this system and have developed alternatives,

such as a non-antibiotic based selection system, for its use by the scientific community. This system has been extensively used to identify genes of interests in the *Anaplasma* spp. and *Ehrlichia chaffeensis*. One such mutant has an insertion within the coding region of the hypothetical protein APH_0906. This protein is important for the replication of the bacteria *in vitro* in HL-60 cells and RF-6 A cells as the number of bacteria does not change over time. Localization of the protein in infected cells confirms its role as an effector that translocates to the cytoplasm of infected cells. Bioinformatic analysis suggests a role in mRNA binding and predicted clear differences between human pathogenic and non-human pathogenic strains.

Appendix A. Supplementary data

Supplementary material related to this article can be found, in the online version, at doi:https://doi.org/10.1016/j.ttbdis.2018.11.006.

References

Absmeier, E., Santos, K.F., Wahl, M.C., 2016. Functions and regulation of the Brr2 RNA helicase during splicing. Cell Cycle 15, 3362–3377. https://doi.org/10.1080/15384101.2016.1249549.

Bao, Y., Tian, M., Li, P., Liu, J., Ding, C., Yu, S., 2017. Characterization of *Brucella abortus* mutant strain Delta22915, a potential vaccine candidate. Vet. Res. 48 (17). https://doi.org/10.1186/s13567-017-0422-9.

Barbet, A.F., Agnes, J.T., Moreland, A.L., Lundgren, A.M., Alleman, A.R., Noh, S.M., Brayton, K.A., Munderloh, U.G., Palmer, G.H., 2005. Identification of functional promoters in the msp2 expression loci of *Anaplasma marginale* and *Anaplasma phagocytophilum*. Gene 353, 89–97. https://doi.org/10.1016/j.gene.2005.03.036.

Barbet, A.F., Al-Khedery, B., Stuen, S., Granquist, E.G., Felsheim, R.F., Munderloh, U.G., 2013. An emerging tick-borne disease of humans is caused by a subset of strains with conserved genome structure. Pathogens 2, 544–555.

Barre, N., Happold, J., Delathiere, J.-M., Desoutter, D., Salery, M., de Vos, A., Marchal, C., Perrot, R., Grailles, M., Mortelecque, A., 2011. A campaign to eradicate bovine babesiosis from New Caledonia. Ticks Tick. Borne. Dis. 2, 55–61. https://doi.org/10.1016/j.ttbdis.2010.11.001.

Beare, P.A., Larson, C.L., Gilk, S.D., Heinzen, R.A., 2012. Two systems for targeted gene deletion in Coxiella burnetii. Appl. Environ. Microbiol. 78, 4580–4589. https://doi.org/10.1128/AEM.00881-12.

Birkner, K., Steiner, B., Rinkler, C., Kern, Y., Aichele, P., Bogdan, C., von Loewenich, F.D., 2008. The elimination of *Anaplasma phagocytophilum* requires CD4+ T cells, but is independent of Th1 cytokines and a wide spectrum of effector mechanisms. Eur. J. Immunol. 38, 3395–3410. https://doi.org/10.1002/eji.200838615.

Burkhardt, N.Y., Baldridge, G.D., Williamson, P.C., Billingsley, P.M., Heu, C.C., Felsheim, R.F., Kurtti, T.J., Munderloh, U.G., 2011. Development of shuttle vectors for transformation of diverse Rickettsia species. PLoS One 6, e29511.

Chávez, A.S.O., Felsheim, R.F., Kurtti, T.J., Ku, P.-S., Brayton, K.A., Munderloh, U.G., 2012. Expression patterns of *Anaplasma marginale* Msp2 variants change in response to growth in cattle, and tick cells versus mammalian cells. PLoS One 7, e36012. https://doi.org/10.1371/journal.pone.0036012.

Chen, G., Severo, M.S., Sakhon, O.S., Choy, A., Herron, M.J., Felsheim, R.F., Wiryawan, H., Liao, J., Johns, J.L., Munderloh, U.G., Sutterwala, F.S., Kotsyfakis, M., Pedra, J.H., 2012. *Anaplasma phagocytophilum* dihydrolipoamide dehydrogenase 1 affects host-

derived immunopathology during microbial colonization. Infect. Immun. 80, 3194–3205.

Cheng, C., Nair, A.D.S., Indukuri, V.V., Gong, S., Felsheim, R.F., Jaworski, D., Munderloh, U.G., Ganta, R.R., 2013. Targeted and random mutagenesis of *Ehrlichia chaffeensis* for the identification of genes required for in vivo infection. PLoS Pathog. 9, e1003171. https://doi.org/10.1371/journal.ppat.1003171.

Cheng, C., Nair, A.D.S., Jaworski, D.C., Ganta, R.R., 2015. Mutations in *Ehrlichia chaffeensis* causing polar effects in gene expression and differential host specificities. PLoS One 10, e0132657. https://doi.org/10.1371/journal.pone.0132657.

Crosby, F.L., Brayton, K.A., Magunda, F., Munderloh, U.G., Kelley, K.L., Barbet, A.F., 2015. Reduced Infectivity in cattle for an outer membrane protein mutant of Anaplasma marginale. Appl. Environ. Microbiol. 81, 2206–2214. https://doi.org/10.1128/AEM.03241-14.

Dahlgren, F.S., Heitman, K.N., Drexler, N.A., Massung, R.F., Behravesh, C.B., 2015. Human granulocytic anaplasmosis in the United States from 2008 to 2012: a summary of national surveillance data. Am. J. Trop. Med. Hyg. 93, 66–72.

Dugat, T., Lagree, A.C., Maillard, R., Boulouis, H.J., Haddad, N., 2015. Opening the black box of *Anaplasma phagocytophilum* diversity: current situation and future perspectives. Front. Cell. Infect. Microbiol. 5, 61.

Dumler, J.S., Sinclair, S.H., Shetty, A.C., 2018. Alternative splicing of differentiated myeloid cell transcripts after infection by *Anaplasma phagocytophilum* impacts a selective group of cellular programs. Front. Cell. Infect. Microbiol. 8, 14. https://doi.org/10.3389/fcimb.2018.00014.

Eremeeva, M.E., Dasch, G.A., 2011. Anaplasmataceae as human pathogens: biology, ecology and epidemiology. Revue Tunisienne d'Infectiologie, Intracellular Bacteria: From Biology to Clinic. pp. S7–S14.

Felsheim, R.F., Chávez, A.S.O., Palmer, G.H., Crosby, L., Barbet, A.F., Kurtti, T.J., Munderloh, U.G., 2010. Transformation of Anaplasma marginale. Vet. Parasitol. 167. https://doi.org/10.1016/j.vetpar.2009.09.018.

Felsheim, R.F., Herron, M.J., Nelson, C.M., Burkhardt, N.Y., Barbet, A.F., Kurtti, T.J., Munderloh, U.G., 2006. Transformation of Anaplasma phagocytophilum. BMC Biotechnol. 6, 42.

Feng, H.-M., Whitworth, T., Olano, J.P., Popov, V.L., Walker, D.H., 2004. Fc-dependent polyclonal antibodies and antibodies to outer membrane proteins A and B, but not to lipopolysaccharide, protect SCID mice against fatal *Rickettsia conorii* infection. Infect. Immun. 72, 2222–2228.

Futse, J.E., Brayton, K.A., Nydam, S.D., Palmer, G.H., 2009. Generation of antigenic variants via gene conversion: evidence for recombination fitness selection at the locus level in Anaplasma marginale. Infect. Immun. 77, 3181–3187. https://doi.org/10.1128/IAI.00348-09.

Goodman, J.L., Nelson, C., Vitale, B., Madigan, J.E., Dumler, J.S., Kurtti, T.J., Munderloh, U.G., 1996. Direct cultivation of the causative agent of human granulocytic ehrlichiosis. N. Engl. J. Med. 334, 209–215.

Hammac, G.K., Ku, P.-S., Galletti, M.F., Noh, S.M., Scoles, G.A., Palmer, G.H., Brayton, K.A., 2013. Protective immunity induced by immunization with a live, cultured *Anaplasma marginale* strain. Vaccine 31, 3617–3622. https://doi.org/10.1016/j.vaccine.2013.04.069.

Herrero, M., de Lorenzo, V., Timmis, K.N., 1990. Transposon vectors containing non-antibiotic resistance selection markers for cloning and stable chromosomal insertion of foreign genes in gram-negative bacteria. J. Bacteriol. 172, 6557–6567.

Herron, M.J., Ericson, M.E., Kurtti, T.J., Munderloh, U.G., 2005. The interactions of *Anaplasma phagocytophilum*, endothelial cells, and human neutrophils. Ann. N. Y. Acad. Sci. 1063, 374–382.

Herron, M.J., Felsheim, R.F., Nelson, C.M., Oliva Chávez, A.S., Munderloh, U.G., 2010. Construction and screening of an *Anaplasma phagocytophilum* mutant library. 24th Meeting of the American Society for Rickettsiology.

Hoerlein, G., 1994. Glufosinate (phosphinothricin), a natural amino acid with unexpected herbicidal properties. Rev. Environ. Contam. Toxicol. 138, 73–145.

Huang, B., Troese, M.J., Ye, S., Sims, J.T., Galloway, N.L., Borjesson, D.L., Carlyon, J.A., 2010. *Anaplasma phagocytophilum* APH_1387 is expressed throughout bacterial intracellular development and localizes to the pathogen-occupied vacuolar membrane. Infect. Immun. 78, 1864–1873.

Kosugi, S., Hasebe, M., Tomita, M., Yanagawa, H., 2009. Systematic identification of cell cycle-dependent yeast nucleocytoplasmic shuttling proteins by prediction of composite motifs. Proc. Natl. Acad. Sci. U. S. A. 106, 10171–10176.

Kumar, S., Stecher, G., Tamura, K., 2016. MEGA7: molecular evolutionary genetics analysis version 7.0 for bigger datasets. Mol. Biol. Evol. 33, 1870–1874.

Lampe, D.J., Grant, T.E., Robertson, H.M., 1998. Factors affecting transposition of the Himar1 mariner transposon in vitro. Genetics 149, 179–187.

Letunic, I., Doerks, T., Bork, P., 2015. SMART: recent updates, new developments and status in 2015. Nucleic Acids Res. 43, D257–D260.

Lin, M., Rikihisa, Y., 2003. *Ehrlichia chaffeensis* and *Anaplasma phagocytophilum* lack genes for lipid A biosynthesis and incorporate cholesterol for their survival. Infect. Immun. 71, 5324–5331.

Lockwood, S., Voth, D.E., Brayton, K.A., Beare, P.A., Brown, W.C., Heinzen, R.A., Broschat, S.L., 2011. Identification of *Anaplasma marginale* type IV secretion system effector proteins. PLoS One 6, e27724. https://doi.org/10.1371/journal.pone.0027724.

Lynn, G.E., Oliver, J.D., Nelson, C.M., Felsheim, R.F., Kurtti, T.J., Munderloh, U.G., 2015. Tissue distribution of the *Ehrlichia muris*-like agent in a tick vector. PLoS One 10, e0122007. https://doi.org/10.1371/journal.pone.0122007.

Majazki, J., Wuppenhorst, N., Hartelt, K., Birtles, R., von Loewenich, F.D., 2013. *Anaplasma phagocytophilum* strains from voles and shrews exhibit specific ankA gene sequences. BMC Vet. Res. 9, 235.

McClure, E.E., Chávez, A.S.O., Shaw, D.K., Carlyon, J.A., Ganta, R.R., Noh, S.M., Wood, D.O., Bavoil, P.M., Brayton, K.A., Martinez, J.J., McBride, J.W., Valdivia, R.H.,

Munderloh, U.G., Pedra, J.H.F., 2017. Engineering of obligate intracellular bacteria: progress, challenges and paradigms. Nat. Rev. Microbiol. 15, 544–558. https://doi.org/10.1038/nrmicro.2017.59.

Meyer, D.F., Noroy, C., Moumene, A., Raffaele, S., Albina, E., Vachiery, N., 2013. Searching algorithm for type IV secretion system effectors 1.0: a tool for predicting type IV effectors and exploring their genomic context. Nucleic Acids Res. 41, 9218–9229. https://doi.org/10.1093/nar/gkt718.

Munderloh, U.G., Felsheim, R.F., Burkhardt, N.Y., Herron, M.J., Oliva Chávez, A.S., Nelson, C.M., Kurtti, T.J., 2012. The way forward: improving genetic systems. Intracellular Pathogens II: Rickettsiales 89, 3.

Munderloh, U.G., Jauron, S.D., Fingerle, V., Leitritz, L., Hayes, S.F., Hautman, J.M., Nelson, C.M., Huberty, B.W., Kurtti, T.J., Ahlstrand, G.G., Greig, B., Mellencamp, M.A., Goodman, J.L., 1999. Invasion and intracellular development of the human granulocytic ehrlichiosis agent in tick cell culture. J. Clin. Microbiol. 37, 2518–2524.

Munderloh, U.G., Lynch, M.J., Herron, M.J., Palmer, A.T., Kurtti, T.J., Nelson, R.D., Goodman, J.L., 2004. Infection of endothelial cells with *Anaplasma marginale* and *A. Phagocytophilum*. Vet. Microbiol. 101, 53–64.

Nelson, C.M., Herron, M.J., Felsheim, R.F., Schloeder, B.R., Grindle, S.M., Chavez, A.O., Kurtti, T.J., Munderloh, U.G., 2008. Whole genome transcription profiling of *Anaplasma phagocytophilum* in human and tick host cells by tiling array analysis. BMC Genomics 9. https://doi.org/10.1186/1471-2164-9-364.

Nguyen Ba, A.N., Pogoutse, A., Provart, N., Moses, A.M., 2009. NLStradamus: a simple Hidden Markov Model for nuclear localization signal prediction. BMC Bioinformatics 10, 202.

Nguyen, T.H., Li, J., Galej, W.P., Oshikane, H., Newman, A.J., Nagai, K., 2013. Structural basis of Brr2-Prp8 interactions and implications for U5 snRNP biogenesis and the spliceosome active site. Structure 21, 910–919.

Noh, S.M., Brayton, K.A., Brown, W.C., Norimine, J., Munske, G.R., Davitt, C.M., Palmer, G.H., 2008. Composition of the surface proteome of *Anaplasma marginale* and its role in protective immunity induced by outer membrane immunization. Infect. Immun. 76, 2219–2226. https://doi.org/10.1128/IAI.00008-08.

Oliva Chávez, A.S., Fairman, J.W., Felsheim, R.F., Nelson, C.M., Herron, M.J., Higgins, L., Burkhardt, N.Y., Oliver, J.D., Markowski, T.W., Kurtti, T.J., Edwards, T.E., Munderloh, U.G., 2015. An O-Methyltransferase is required for infection of tick cells by Anaplasma phagocytophilum. PLoS Pathog. 11, e1005248. https://doi.org/10.1371/journal.ppat.1005248.

Peng, Z., Kurgan, L., 2015. High-throughput prediction of RNA, DNA and protein binding regions mediated by intrinsic disorder. Nucleic Acids Res. 43, e121.

Plaschka, C., Lin, P.-C., Nagai, K., 2017. Structure of a pre-catalytic spliceosome. Nature 546, 617–621. https://doi.org/10.1038/nature22799.

Pritt, B.S., Allerdice, M.E.J., Sloan, L.M., Paddock, C.D., Munderloh, U.G., Rikihisa, Y., Tajima, T., Paskewitz, S.M., Neitzel, D.F., Hoang Johnson, D.K., Schiffman, E., Davis, J.P., Goldsmith, C.S., Nelson, C.M., Karpathy, S.E., 2017. Proposal to reclassify *Ehrlichia muris* as *Ehrlichia muris* subsp. *Muris* subsp. Nov. And description of *Ehrlichia muris* subsp. *Eauclairensis* subsp. nov., a newly recognized tick-borne pathogen of humans. Int. J. Syst. Evol. Microbiol. 67, 2121–2126. https://doi.org/10.1099/ijsem.0.001896.

ProMED-Mail, 2017. PRO/AH/EDR& Invasive tick – USA: (NJ) [WWW Document]. Arch. Number 20171123.5462146. URL http://www.promedmail.org/post/5462146 (Accessed 23 November 2017).

Rikihisa, Y., 2011. Mechanisms of obligatory intracellular infection with Anaplasma phagocytophilum. Clin. Microbiol. Rev. 24, 469–489. https://doi.org/10.1128/CMR.00064-10.

Robinson, S.J., Neitzel, D.F., Moen, R.A., Craft, M.E., Hamilton, K.E., Johnson, L.B., Mulla, D.J., Munderloh, U.G., Redig, P.T., Smith, K.E., Turner, C.L., Umber, J.K., Pelican, K.M., 2015. Disease risk in a dynamic environment: the spread of tick-borne pathogens in Minnesota, USA. Ecohealth 12, 152–163. https://doi.org/10.1007/s10393-014-0979-y.

Santos, K.F., Jovin, S.M., Weber, G., Pena, V., Luhrmann, R., Wahl, M.C., 2012. Structural basis for functional cooperation between tandem helicase cassettes in Brr2-mediated remodeling of the spliceosome. Proc. Natl. Acad. Sci. U. S. A. 109, 17418–17423.

Scharf, W., Schauer, S., Freyburger, F., Petrovec, M., Schaarschmidt-Kiener, D., Liebisch, G., Runge, M., Ganter, M., Kehl, A., Dumler, J.S., Garcia-Perez, A.L., Jensen, J., Fingerle, V., Meli, M.L., Ensser, A., Stuen, S., von Loewenich, F.D., 2011. Distinct host species correlate with *Anaplasma phagocytophilum* ankA gene clusters. J. Clin. Microbiol. 49, 790–796.

Schotthoefer, A.M., Schrodi, S.J., Meece, J.K., Fritsche, T.R., Shukla, S.K., 2017. Pro-inflammatory immune responses are associated with clinical signs and symptoms of human anaplasmosis. PLoS One 12, e0179655. https://doi.org/10.1371/journal.pone.0179655.

Sinclair, S.H., Garcia-Garcia, J.C., Dumler, J.S., 2015. Bioinformatic and mass spectrometry identification of *Anaplasma phagocytophilum* proteins translocated into host cell nuclei. Front. Microbiol. 6, 55.

Thirumalapura, N.R., Crossley, E.C., Walker, D.H., Ismail, N., 2009. Persistent infection contributes to heterologous protective immunity against fatal ehrlichiosis. Infect. Immun. 77, 5682–5689. https://doi.org/10.1128/IAI.00720-09.

Thompson, C.J., Movva, N.R., Tizard, R., Crameri, R., Davies, J.E., Lauwereys, M., Botterman, J., 1987. Characterization of the herbicide-resistance gene bar from *Streptomyces hygroscopicus*. EMBO J. 6, 2519–2523.

Tian, T., Salis, H.M., 2015. A predictive biophysical model of translational coupling to coordinate and control protein expression in bacterial operons. Nucleic Acids Res. 43, 7137–7151. https://doi.org/10.1093/nar/gkv635.

Troese, M.J., Carlyon, J.A., 2009. *Anaplasma phagocytophilum* dense-cored organisms mediate cellular adherence through recognition of human P-selectin glycoprotein ligand 1. Infect. Immun. 77, 4018–4027.

Valbuena, G., Jordan, J.M., Walker, D.H., 2004. T cells mediate cross-protective

immunity between spotted fever group rickettsiae and typhus group rickettsiae. J. Infect. Dis. 190, 1221–1227. https://doi.org/10.1086/423819.

Wang, Y., Wei, L., Liu, H., Cheng, C., Ganta, R.R., 2017. A genetic system for targeted mutations to disrupt and restore genes in the obligate bacterium, Ehrlichia chaffeensis. Sci. Rep. 7, 15801. https://doi.org/10.1038/s41598-017-16023-y.

Wu, S., Zhang, Y., 2007. LOMETS: a local meta-threading-server for protein structure prediction. Nucleic Acids Res. 35, 3375–3382.

Yang, J., Liu, Z., Niu, Q., Liu, J., Xie, J., Chen, Q., Chen, Z., Guan, G., Liu, G., Luo, J., Yin, H., 2016. Evaluation of different nested PCRs for detection of *Anaplasma phagocytophilum* in ruminants and ticks. BMC Vet. Res. 12 (35). https://doi.org/10.1186/s12917-016-0663-2.